

# Tailoring the magnetic properties and magnetorheological behavior of spinel nanocrystalline cobalt ferrite by annealing temperature

*Michal Sedlacik<sup>a,b,\*</sup>, Vladimir Pavlinek<sup>a,c</sup>, Petra Peer<sup>d</sup>, Petr Filip<sup>d</sup>*

<sup>a</sup>Centre of Polymer Systems, University Institute, Tomas Bata University in Zlin, Nad Ovcirnou 3685, 760 01, Zlin, Czech Republic

<sup>b</sup>Department of Production Engineering, Faculty of Technology, Tomas Bata University in Zlin, T. G. Masaryk Sq. 275, 762 72, Zlin, Czech Republic

<sup>c</sup>Polymer Centre, Faculty of Technology, Tomas Bata University in Zlin, T. G. Masaryk Sq. 275, 762 72, Zlin, Czech Republic

<sup>d</sup>Institute of Hydrodynamics, Academy of Sciences of the Czech Republic, Pod Patankou 5, 166 12 Prague 6, Czech Republic

\*Corresponding author: Centre of Polymer Systems, University Institute, Tomas Bata University in Zlin, Nad Ovcirnou 3685, 760 01, Zlin, Czech Republic. Tel.: +420 57 603 8027; fax: +420 57 603 1444; E-mail: msedlacik@ft.utb.cz

## ABSTRACT

Magnetic nanoparticles of spinel nanocrystalline cobalt ferrite were synthesized via the sol–gel method and subsequent annealing. The influence of the annealing temperature on the structure, magnetic properties, and magnetorheological effect was investigated. The finite crystallite size of particles determined by X–ray diffraction as well as particle size observed via transmission electron microscopy increased with annealing temperature. The magnetic properties observed via vibrating sample magnetometer showed that an increase in the annealing temperature leads to the increase in the magnetization saturation and, in contrast, a decrease in coercivity. The effect of annealing on magnetic properties of ferrite particles has been explained by the recrystallization process at high temperature resulting in grain size growth and decrease in an imposed stress relating to defects of crystal lattice structure of nanoparticles. The magnetorheological characteristics of suspensions of ferrite particles in silicone oil were measured using a rotational rheometer equipped with a magnetic field generator in both steady shear and small–strain oscillatory regime. The magnetorheological performance expressed as a relative increase in magnetoviscosity appeared to be significantly higher for suspensions of particles annealed at 1000 °C.

## Keywords

Magnetorheology; Magnetoviscosity; Spinel nanocrystalline cobalt ferrite; Sol–gel synthesis; Annealing temperature; Recrystallization

## 1. Introduction

Magnetorheological (MR) suspensions belong to a class of smart materials which typically consist of magnetizable micron-sized particles dispersed in non-magnetic liquids

which in the presence of a magnetic field evince rapid change in their rheological properties [1]. When an external magnetic field is applied to such systems with randomly distributed particles, the magnetic dipoles of particles align parallel to the external field, resulting in a particle chain-like structure. In the flow field, the shear stress increases and even a yield stress may appear. When the magnetic field is switched off, the particle chains are destroyed due to shear forces and the shear stress rapidly decreases. A fast change in the rheological properties of MR suspensions in response to a magnetic field offers the possibility to use this phenomenon in technical applications such as clutches, control valves, shock absorbers, torque transducers, dampers, polishing fluids or various medical applications [2–6].

Spinel cobalt ferrite ( $\text{CoFe}_2\text{O}_4$ ) ranks among promising materials as a dispersed phase for magneto-sensitive systems. It exhibits moderate saturation magnetization as well as excellent chemical stability. Several methods have been proposed for the preparation of this material with various magnetic properties, such as co-precipitation [7], oxidation [7], hydrothermal [8] or sol–gel synthesis [9–10].

The sol–gel technique proved to be an attractive method due to its homogeneous reactant distribution resulting in both a uniform particle shape and a highly crystalline quality of the product [11]. The nanoparticles of the  $\text{CoFe}_2\text{O}_4$  prepared via this method have been used to demonstrate the effect of annealing temperature on the magnetorheological efficiency of their silicone oil suspensions in the present study.

## **2. Experimental Section**

### **2.1 Materials**

Iron(III) nitrate nonahydrate  $\text{Fe}(\text{NO}_3)_3 \cdot 9\text{H}_2\text{O}$ , cobalt acetate tetrahydrate  $\text{Co}(\text{CH}_3\text{CO}_2)_2 \cdot 4\text{H}_2\text{O}$ , and 2-methoxyethanol used for the synthesis of cobalt ferrite were all of reagent grade and purchased from Sigma–Aldrich (USA).

## **2.2 Preparation of CoFe<sub>2</sub>O<sub>4</sub> Nanoparticles**

1/100 mol Fe(NO<sub>3</sub>)<sub>3</sub>·9H<sub>2</sub>O and 1/200 mol Co(CH<sub>3</sub>CO<sub>2</sub>)<sub>2</sub>·4H<sub>2</sub>O were dissolved in 100 ml 2-methoxyethanol with 15 ml of distilled water. The mixture was ultrasonicated for 30 min and then refluxed at 70 °C for 12 h. The formed gel was dried at 100 °C and ground in a ball mill (Retsch MM301, Retsch GmbH, Germany). Despite our earlier report [12], the powder was then heated from the laboratory temperature at the rate of 1°C min<sup>-1</sup> to the annealing temperature 400 °C, 850 °C or 1000 °C which was maintained for 3 h and corresponding density of so-prepared particles obtained via gas pycnometer (Upyc 1200e, Quantachrome, USA) was 5.3287, 5.3034, and 5.2962 g/cm<sup>3</sup>, respectively. The prepared CoFe<sub>2</sub>O<sub>4</sub> particles were then sieved to obtain particle sizes lower than 45 μm.

## **2.3 Particle Structure Characterization**

The X-ray diffraction (XRD) patterns of the CoFe<sub>2</sub>O<sub>4</sub> particles were analyzed with an X'Pert PRO X-ray diffractometer (Philips, the Netherlands) with CuKα radiation (λ = 0.154 nm) in reflection mode and 2θ ranging from 25° to 70°.

Figure 1 illustrates the XRD diffraction patterns of all three samples. It is worth noting here that different times of annealing were examined, but the resulting patterns were approximately the same and thus only the time of 3 h was used. All the diffraction peaks can be indexed to the face centre structure of CoFe<sub>2</sub>O<sub>4</sub> according to JCPDS card No. 22-1086 and JCPDS card No. 01-1121. In the XRD patterns no impurity peaks were detected. The most intensive peak (311) confirms the formation of a cubic spinel structure of the prepared material. In addition, an increase in intensity of the major peaks implies that the crystallites formed have higher quality resulting subsequently in their increased size along with increasing annealing temperature. Based on the Scherrer formula,

$$D = 0.9\lambda / \beta \cos\theta \quad (1)$$

where  $D$  is the finite crystallite size,  $\lambda$  is the wavelength of anode  $\text{CuK}\alpha$ ,  $\beta$  is the full width at half maxima (FWHM) of the diffraction peak, and  $\theta$  is the Bragg's angle. Thereafter, the crystallite sizes of  $\text{CoFe}_2\text{O}_4$  powders were estimated to be 30 nm, 65 nm, and 82 nm for particles annealed at 400 °C, 850 °C and 1000 °C, respectively.

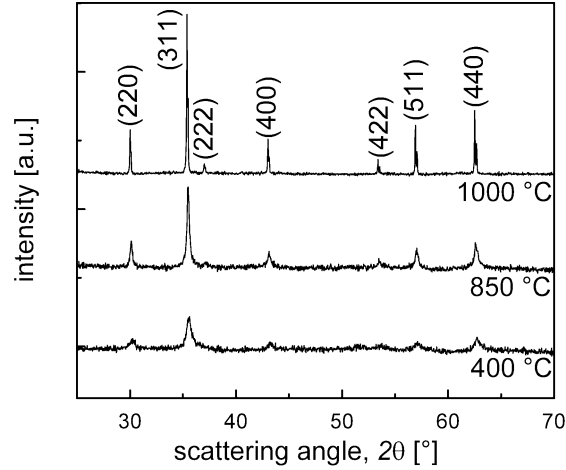


Fig. 1. X-ray diffraction patterns of the  $\text{CoFe}_2\text{O}_4$  particles obtained at various annealing temperatures.

The changes in  $\text{CoFe}_2\text{O}_4$  particle size resulting from the use of different annealing temperatures were determined using a JEOL 1200 (JEOL Ltd, Japan) transmission electron microscope (TEM). As can be seen in Fig. 2, all particles are polyhedral, rather forming agglomerates than single particles. The increase in annealing temperature yielded larger single  $\text{CoFe}_2\text{O}_4$  particles. Moreover, the increase of temperature up to 1000 °C leads to the formation of particles with the size corresponding to multi-domain state for  $\text{CoFe}_2\text{O}_4$  ( $d_{\text{cr}} > 100$  nm [13]) as a result of the recrystallization process when the grain growth is accomplished by the replacement of original deformed crystallites by un-deformed one.. However, recrystallization leads to a polycrystalline behavior of particles and a wide distribution of particle sizes as it is confirmed by TEM results (Fig. 2c).

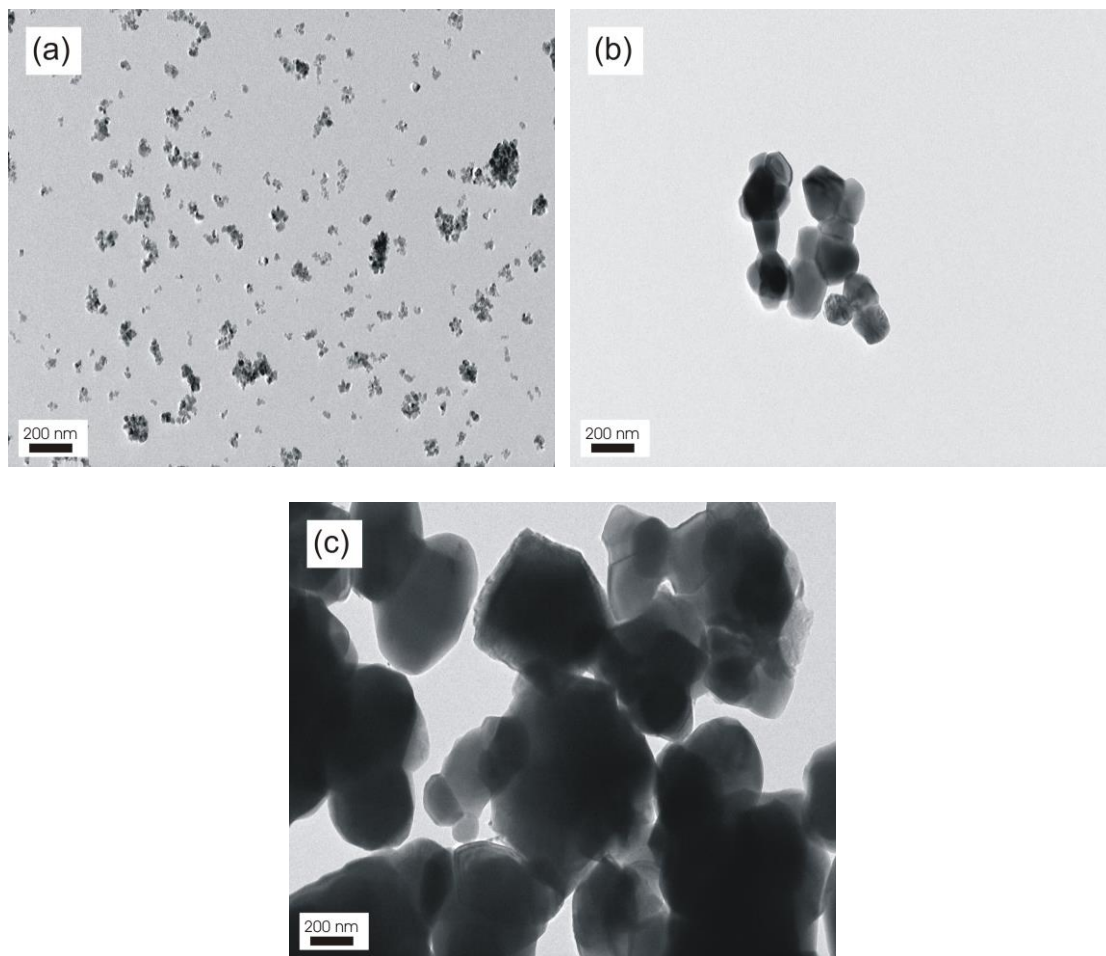


Fig. 2. TEM images of the  $\text{CoFe}_2\text{O}_4$  particles annealed at: a) 400 °C; b) 850 °C; c) 1000 °C.

## **2.4 The Magnetic Properties**

The magnetic properties of the samples were measured at room temperature using a vibrating sample magnetometer (VSM, Lakeshore, USA) at the magnetic field of 12 kOe. Magnetic hysteresis loops of annealed  $\text{CoFe}_2\text{O}_4$  are shown in Fig. 3. Changes in the magnetic properties of particles are caused by a different micromagnetic structure of nanoparticles which is indirectly associated with the crystallite size depending on the annealing temperature. The higher the annealing temperature, the higher is magnetization saturation: 36, 63, and 78  $\text{emu g}^{-1}$  for 400 °C, 850 °C and 1000 °C annealing temperature, respectively. Furthermore, the remanence to magnetization saturation ratio is 0.6 for particles annealed at 850 °C, indicating randomly oriented equiaxial crystallites with cubic magnetocrystalline anisotropy in the system [14]. On the other hand, the lower the annealing temperature used, the higher the coercivity, i.e. the coercivity of annealed particles 1725, 728, and 298 Oe decreases along with the annealing temperature. The decrease of the coercivity with increase of annealing temperature is also determined by micromagnetic structure and particle size, more precisely

with the magnetic state of the particle, namely superparamagnetic or ferromagnetic. It is known, that with decrease of particle size the coercivity increases to its maximum which corresponds to the transition between multi-domain to single-domain state [15]. It is explained by the increased value of effective magnetic anisotropy in single-domain particles due to the contribution of shape and surface anisotropy, as well as anisotropy of imposed stress relating to defects of crystal lattice structure of nanoparticles. Thus, the increased coercivity in the samples can be attributed to the large residual strains and possible defects in the spinel nanocrystalline  $\text{CoFe}_2\text{O}_4$  powders caused by grinding during their preparation. Therefore, the high magnetization saturation and low coercivity of sample annealed at 1000 °C temperature made it suitable for practical application in MR, since minimal or no coercivity of dispersed magnetic particles does not lead to the undesirable heating of the MR system under periodic cycling.

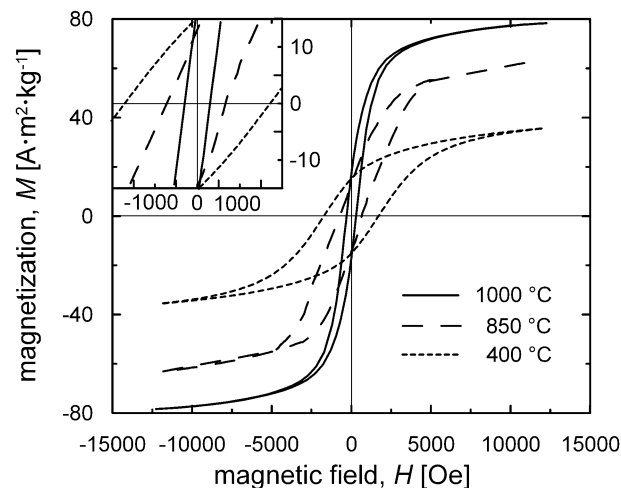


Fig. 3. Hysteresis loops of ferrite samples at room temperature; inset – the course at low magnetic field.

## 2.5 Suspension Preparation

20, 40, and 60 wt.% suspensions of the ferrite samples in silicone oil (Lukosiol M15, Chemical Works Kolín, Czech Republic; viscosity of 14.5 mPa s, density of  $0.965 \text{ g cm}^{-3}$ ) were prepared. 0.5 wt.% of nano-silica (average particles size  $\sim 10 \text{ nm}$ , Aerosil A 200, Degusa, Germany) was added to suspensions in order to enhance the sedimentation stability [16]. All prepared suspensions formed well-dispersed systems for the period of the experiment.

## **2.6 Magnetorheological Measurement**

The MR properties of suspensions under investigation were measured using a rotational rheometer Physica MCR501 (Anton Paar GmbH, Austria) with a Physica MRD 180/1T magneto-cell at 25 °C. True magnetic flux density (0 – 300 mT) was measured using a Hall probe, and temperature was checked with the help of an inserted thermocouple. Both the Hall probe and the thermocouple were housed in the bottom plate; for details see [17]. A parallel-plate measuring system with a diameter of 20 mm and gap of 1 mm was used. All steady shear flow measurements were performed under controlled shear rate mode in the shear rate range 0.1 – 300 s<sup>-1</sup> in a log scale with 6 pts/decade. The small-strain oscillatory tests were carried out through dynamic strain sweeps and frequency sweeps. The strain sweeps were performed in the applied strain range of 10<sup>-5</sup> to 0.1 at a fixed angular frequency of 62.8 rad s<sup>-1</sup> under a magnetic field in order to get the position of the linear viscoelastic region (LVR). Afterwards, the viscoelastic moduli were obtained from frequency sweep tests (0.628 to 62.8 rad s<sup>-1</sup>) at a fixed strain amplitude in the LVR ( $\gamma = 2 \times 10^{-5}$  in our experiments). In both modes before each measurement at a new magnetic field, the residual internal structures were destroyed by continuous shearing ( $\dot{\gamma} = 100 \text{ s}^{-1}$ ) for 1 min. Each measurement under given conditions was performed three times and the average value was used for further evaluation. The temperature was maintained at 25 °C. Prior to the measurement every suspension was mechanically stirred.

## **3. Results and Discussion**

### **3.1 Flow Behavior at Steady Shear**

Figure 4 depicts the MR activity of three systems differing in the annealing temperature of the samples obtained from the steady shear test. An almost linear log – log plot of the shear stress vs. shear rate for the suspension of particles annealed at 850 °C and 1000 °C in the absence of a magnetic field indicates nearly Newtonian behavior characteristics. At the same



time, the particle loading viscosity of the suspension of the particles annealed at 400 °C dominates the others, probably due to smaller  $\text{CoFe}_2\text{O}_4$  particles. A noticeable increase in the shear stress and viscosity in the magnetic field is caused by the formation of an internal particle chain-like structure. The shear stress steeply increases as the liquid suspension changes to a solid-like state and a yield stress can be detected. Its value, obtained by extrapolation of the shear stress to the zero shear rate, increased along with the annealing temperature. It is clear that a more developed domain structure of particles annealed at higher temperatures results in a higher value of magnetization (Fig. 3), which in turn results in a stiffer particle chain-like structure in a magnetic field.

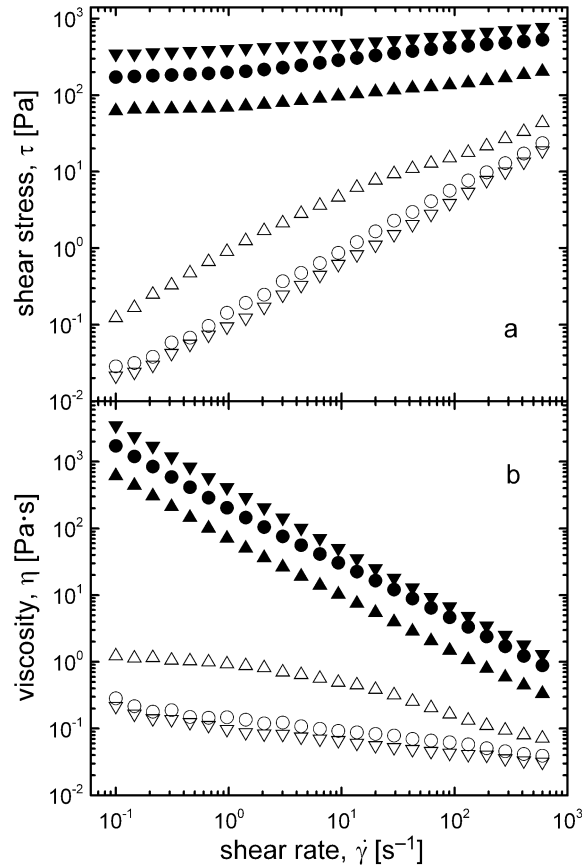


Fig. 4. Double-logarithmic plots of the shear stress,  $\tau$ , (a) and the viscosity,  $\eta$ , (b) vs. shear rate,  $\dot{\gamma}$ , for 40 wt.% suspension of cobalt ferrite particles annealed at 400 °C ( $\blacktriangle, \triangle$ ), 850 °C ( $\bullet, \circ$ ) and 1000 °C ( $\blacktriangledown, \triangledown$ ) under 0 mT (open symbols) and 265 mT (solid symbols).

Similarly to electrorheological fluids [18], the performance of MR suspension may be significantly affected by field-off behavior. Thus, a relative increase in magnetoviscosity,  $\Delta\eta_M = \eta_M - \eta_0$ , expressed as  $e = (\eta_M - \eta_0)/\eta_0$ , where  $\eta_M$  is the viscosity of a formed MR structure and  $\eta_0$  is the field-off, characterizes a real effectiveness of the system. Figure 5 shows that the most efficient system is based on particles annealed at 1000 °C and at lower annealing temperatures the MR performance of suspensions decreased.

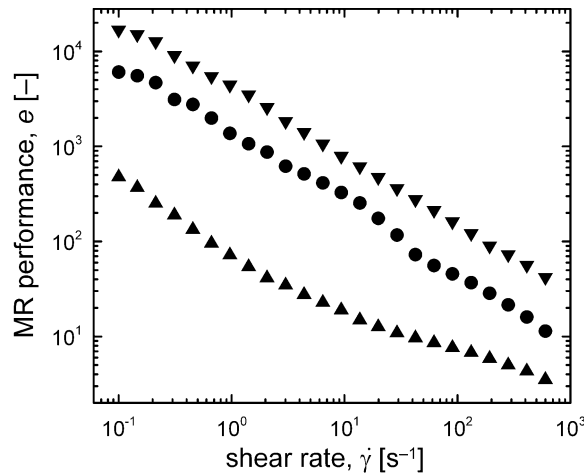


Fig. 5. The dependence of MR performance,  $e$ , at 265 mT on the shear rate,  $\dot{\gamma}$ , for 40 wt.% suspension of cobalt ferrite particles annealed at 400 °C (▲), 850 °C (●) and 1000 °C (▼).

To observe the increase in rigidity of formed internal structures with particle concentration, the shear stress at low shear rate is plotted as a function of the magnetic flux density (Fig. 6). It is evident that a steep increase in the shear stress with the particle concentration under various magnetic flux densities demonstrates a stiffer chain-like structure formation. The stress in all cases firstly increase with the external magnetic field following the square dependence of the magnetic flux density, i.e.  $\tau_{\dot{\gamma}=0.2} = B^2$ , which correlates very well with numerical and analytical models at low magnetic field [18]. Then, the slope of the dependence decreases as the local saturation of magnetic particles occurs with increasing magnetic field. This phenomenon is less pronounced at higher particle concentration since the magnetization is distributed among more particles.

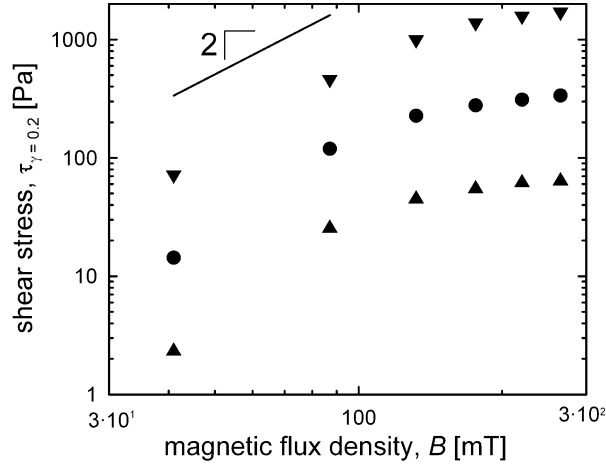


Fig. 6. Shear stress at the shear rate  $\dot{\gamma} = 0.2 \text{ s}^{-1}$ ,  $\tau_{\dot{\gamma}=0.2}$ , dependence on magnetic flux density,  $B$ , for suspensions of cobalt ferrite particles annealed at  $1000 \text{ }^\circ\text{C}$  with various particle concentrations (wt.%): (▲) 20; (●) 40; (▼) 60.

### 3.2 Viscoelastic Properties

The formation of particle chain-like structures in MR suspensions under an external magnetic field also considerably influences the elasticity of the system. Figure 7 illustrates storage,  $G'$ , and loss,  $G''$ , moduli as a function of angular frequency,  $\omega$ , for 60 wt.% suspension of ferrite particles annealed at  $1000 \text{ }^\circ\text{C}$ . In the absence of a magnetic field,  $G'$  predominates over  $G''$  only slightly in the whole angular frequency range probably due to the high interaction of hydrophilic particles non-compatible with the hydrophobic oil matrix.

However, when the magnetic field was applied, as a result of the high elasticity of the particle chain-like structure,  $G'$  dramatically increased and prevailed over  $G''$  throughout the entire frequency range. Elasticity increases with increasing magnetic flux density which can be explained by the formation of more robust chains [19].

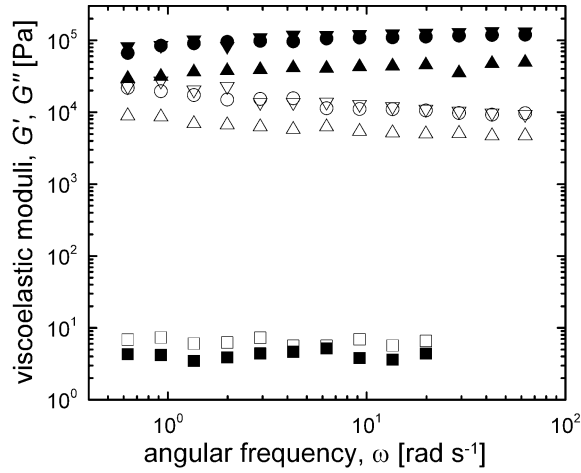


Fig. 7. Storage,  $G'$ , (solid) and loss,  $G''$ , (open) moduli as a function of angular frequency,  $\omega$ , for 60 wt.% suspension of cobalt ferrite particles annealed at 1000 °C. Magnetic flux densities (mT): (■, □) 0; (▲, △) 89; (●, ○) 181; (▼, ▽) 265.

Figure 8 demonstrates that the low-frequency elastic modulus  $G'$  increases nearly linearly with increasing magnetic flux density, which is in good agreement with the theoretical prediction for the influence of a moderate magnetic field in which the contact regions of each particle are saturated [20].

Similarly to the steady shear flow experiments, stronger chain structuralization within the system, and thus higher elastic properties, are observed in suspension of ferrite particles annealed at 1000 °C. The stiffness of the internal structure decreases with decreasing annealing temperature due to the lower magnetization saturation of the particles.

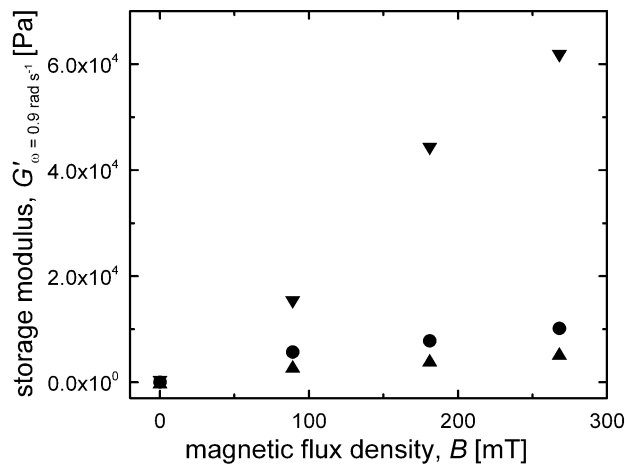


Fig. 8. Storage modulus,  $G'$ , dependence on magnetic flux density,  $B$ , at the angular frequency  $\omega = 0.9 \text{ rad s}^{-1}$  for suspensions of cobalt ferrite particles annealed at 400 °C ( $\blacktriangle$ ), 850 °C ( $\bullet$ ), and 1000 °C ( $\blacktriangledown$ ).

## 4. Conclusions

Annealing temperature at about 850–1000°C proved to be a responsive tool for controlling the magnetic properties of  $\text{CoFe}_2\text{O}_4$  nanoparticles prepared via the sol–gel method. An X–ray diffraction analysis revealed the formation of a spinel phase and an increase in finite crystallite size with increasing annealing temperature. The saturation magnetization and coercivity are proportional to the grain size and, consequently, to the particles size. These properties enabled an adjustment to the optimal magnetorheological behavior of the oil suspension of this material by annealing the particles at a suitable temperature. Thus, a higher magnetoviscoelasticity has been reached for particles annealed at a higher temperature (1000°C) when particles with multi-domain structure are formed.

## Acknowledgements

The authors would like to thank the Grant Agency of the Czech Republic (202/09/1626) for financial support.

This article was written with the support of Operational Programme Research and Development for Innovations co-funded by the European Regional Development Fund (ERDF) and national budget of the Czech Republic, within the framework of the project Centre of Polymer Systems (reg. number: CZ.1.05/2.1.00/03.0111).

## References

- [1] F.F. Fang, H.J. Choi, Y. Seo, *ACS Appl. Mater. Interfaces* 2 (2010) 54–60.
- [2] P. Kuzhir, G. Bossis, V. Bashtovoi, *Int. J. Mod. Phys. B* 19 (2005) 1229–1235.
- [3] M. Sedlacik, R. Moucka, Z. Kozakova, N.E. Kazantseva, V. Pavlinek, I. Kuritka, O. Kaman, P. Peer, *J. Magn. Magn. Mater.* 326 (2013) 7–13.

- [4] Y.D. Liu, J. Lee, S.B. Choi, H.J. Choi, *Smart Mater. Struct.* 22 (2013) 065022.
- [5] S. Jha, V.K. Jain, *Int. J. Adv. Manuf. Technol.* 42 (2009) 656–668.
- [6] I. Bica, *J. Magn. Magn. Mater.* 241 (2002) 196–200.
- [7] M. Feder, L. Diamandescu, I. Bibicu, O.F. Caltun, I. Dumitru, L. Boutiuc, H. Chiriac, N. Lupu, V. Vilceanu, M. Vilceanu, *IEEE Trans. Magn.* 44 (2008) 2936–2939.
- [8] D. Zhao, X. Wu, H. Guan, E. Han, *J. Supercrit. Fluids* 42 (2007) 226–233.
- [9] J. Lee, J.Y. Park, C.S. Kim, *J. Mater. Sci.* 33 (1998) 3965–3968.
- [10] L.H. Ai, J. Jiang, *Curr. Appl. Phys.* 10 (2010) 284–288.
- [11] C.J. Brinker, G.W. Scherer, In *Sol–gel science: The physics and chemistry of sol–gel processing*; Academic Press, Inc.: San Diego, 1990.
- [12] M. Sedlacik, V. Pavlinek, P. Saha, P. Svracinova, P. Filip, *Mod. Phys. Lett. B* 26 (2012) 1150013.
- [12] A.E. Berkowitz, In *Magnetism and Metallurgy*; Academic Press, Inc.: New York, 1969.
- [13] K.M. Krishnan, A.B. Pakhomov, Y. Bao, P. Blomqvist, Y. Chun, M. Gonzales, K. Griffin, X. Ji, B.K. Roberts, *J. Mater. Sci.* 41 (2006) 793–815.
- [14] S.T. Lim, M.S. Cho, I.B. Jang, H.J. Choi, *J. Magn. Magn. Mater.* 282 (2004) 170–173.
- [15] J.M.D. Coey, In *Magnetism and magnetic materials*, Cambridge University Press, Cambridge, UK, 2010.
- [16] Y.D. Liu, Y.H. Li, C.S. Kim, H.J. Choi, *IEEE Trans. Magn.* 49 (2013) 3406–3409.
- [17] M.H. Laun, C. Gabriel, *Rheol. Acta* 46 (2007) 665–676.
- [18] A. Lengalova, V. Pavlinek, P. Saha, O. Quadrat, T. Kitano, J. Stejskal, *Eur. Polym. J.* 39 (2003) 641–645.
- [19] J. de Vicente, M. Lopez–Lopez, F. Gonzales–Caballero, J.D.G. Duran, *J. Rheol.* 47 (2003) 1093–1109.

[20] J.M. Ginder, L.C. Davis, L.D. Elie, , Int. J. Mod. Phys. B 10 (1996) 3293–3303.